Asymptotic observability of low-dimensional powder chaos in a three-degrees-of-freedom scattering system

Gábor Drótos,[1,2,*] Francisco González Montoya,[3] Christof Jung,[3] and Tamás Tél[1,2]
[1]*Institute for Theoretical Physics, Eötvös University, Pázmány Péter sétány 1/A, H-1117 Budapest, Hungary*
[2]*MTA-ELTE Theoretical Physics Research Group, Pázmány Péter sétány 1/A, H-1117 Budapest, Hungary*
[3]*Instituto de Ciencias Físicas, Universidad Nacional Autónoma de México, Av. Universidad s/n, 62251 Cuernavaca, Mexico*
(Received 14 May 2014; published 12 August 2014)

We treat a chaotic Hamiltonian scattering system with three degrees of freedom where the chaotic invariant set is of low dimension. Then the chaos and its structure are not visible in scattering functions plotted along one-dimensional lines in the set of asymptotic initial conditions. We show that an asymptotic observer can nevertheless see the structure of the chaotic set in an appropriate scattering function on the two-dimensional impact parameter plane and in the doubly differential cross section. Rainbow singularities in the cross section carry over the symbolic dynamics of the chaotic set into the cross section. A smooth image of the fractal structure of the chaotic set can be reconstructed on the domain of the cross section.

DOI: 10.1103/PhysRevE.90.022906 PACS number(s): 05.45.−a

I. INTRODUCTION

Chaotic scattering with two degrees of freedom is well studied, and we have a simple recipe to detect the chaos and to observe its properties. We scan asymptotic initial conditions along some appropriate one-dimensional line and monitor the singularities of scattering functions along this line. The resulting fractal pattern reflects the fractal structure of the chaotic invariant set of the system and allows a reconstruction of the important properties of the chaotic set (for general information on chaotic scattering see the recent review [1]). This method works because the singularities are caused by the intersections of the line of initial conditions with the fractal bundle of stable manifolds of the chaotic set, and this bundle contains the information on the fractal structure of the chaotic set itself. We can consider this reconstruction from asymptotic observations as the inverse chaotic scattering problem [2].

In Ref. [3] it has been observed that this simple method does not work with more degrees of freedom. Then in cases of a chaotic set of low dimension the intersection of the stable manifold of the chaotic set with the set of asymptotic initial conditions is of low dimension, in particular if the stable manifold's codimension is larger than one. Then a line of initial conditions in a general position does not intersect the stable manifold at all. This observation appears to be well known and might be interpreted as an argument that chaotic sets of low dimension (high codimension) are not observable at all for an asymptotic observer. The purpose of the present article is to show that this is not so. In such a case, too, the asymptotic observer can obtain the relevant information on the chaotic set.

The first idea is to study scattering functions. When dealing with an autonomous system with n degrees of freedom, then a relevant scattering function to be studied is one defined on an $(n-1)$-dimensional domain. We will show how the fractal pattern of the chaotic set is contained in such a scattering function. A lot more interesting is to study the $(n-1)$-fold differential cross section, since this is the quantity usually obtained in scattering experiments. In the case of chaotic scattering off smooth potentials this quantity contains a set of rainbow singularities which is expected to reflect the fractal structure of the chaotic set. The main topic of the present article is to explain this idea in detail, to demonstrate that asymptotic observations contain information on the chaotic set, and to show how we also recover this information in the case of a chaotic set of low dimension.

In Ref. [3], as an example of demonstration, a billiard system has been used consisting of four hard spheres located on the corners of a tetrahedron. In order to maintain the connection with Ref. [3] we use a soft potential version of the tetrahedron system, similar in spirit to the one studied in Ref. [4]. On the one hand this gives the possibility to compare our results to the hard sphere tetrahedron systems used by Ref. [3] and Refs. [5–12]. On the other hand a smooth potential guarantees a generic form of the rainbow singularities in the differential cross section. More generally it avoids some nongeneric nasty properties of billiard systems.

The organization of our article is as follows. In Sec. II we present the model in detail and give the natural symbolic description of the trajectories. In Sec. III we define the scattering function that is relevant for our argumentation and in particular show how the scattering function naturally cuts its domain into partition cells belonging to the symbolic description of the trajectories constructed in Sec. II. In Sec. IV we study the doubly differential cross section and in particular its rainbow singularities. We will see that these rainbow singularities carry over the symbolic dynamics to the cross section and make it visible for the asymptotic observer. Section V gives considerations of the dimensions of various relevant fractals appearing in chaotic scattering in a general form. In Sec. VI we summarize and discuss the results.

II. THE MODEL AND THE SYMBOLIC DESCRIPTION OF TRAJECTORIES

As a model of demonstration we use a soft potential version of the tetrahedron system, i.e., a total potential consisting of four repulsive potential hills centered at the corners $\mathbf{r}_j, j = 1,2,3,4$ of a tetrahedron. Our particular choice of the potential function V is

$$V(\mathbf{r}) = V_0 \sum_{j=1}^{4} f(|\mathbf{r} - \mathbf{r}_j|) \tag{1}$$

*Corresponding author: drotos@general.elte.hu

where we use $V_0 = 0.08$ and

$$f(z) = \exp(-z^6). \tag{2}$$

This potential hill is intended to approximate rather well a hard sphere. The power 6 in the exponent ensures the potential hill to be still smooth on the one hand, and to fall off sufficiently fast to have an effective radius (i.e., e-fold decaying distance) close to 1 on the other hand. The center of the tetrahedron is placed into the origin of the coordinate system. The corners of the tetrahedron are given by

$$\mathbf{r}_1 = l(1,0,-1/(2\sqrt{2})), \tag{3a}$$

$$\mathbf{r}_2 = l(-1/2,\sqrt{3}/2,-1/(2\sqrt{2})), \tag{3b}$$

$$\mathbf{r}_3 = l(-1/2,-\sqrt{3}/2,-1/(2\sqrt{2})), \tag{3c}$$

$$\mathbf{r}_4 = l(0,0,3/(2\sqrt{2})), \tag{3d}$$

where l is a free parameter to adjust the ratio of the distance between the four potential hills with respect to the effective radius of the potential hills. Later in the numerical examples we set it to the value $l = 3$. On the one hand, we want to set l sufficiently large to avoid too much overlap of the four potential hills and to guarantee a symbolic dynamics with a branching ratio 3. On the other hand, we want to avoid an unnecessarily large value of l, which would cause an extremely large scaling factor in the fractal structure to be investigated.

If the parameter l is chosen appropriately ($l = 3$ is such a case), then the system has unstable periodic trajectories bouncing between the various potential hills in any order with the only restriction that bounce number $i+1$ is off a different hill than bounce number i. Then it is natural to assign to each potential hill a symbol; in particular, we give the label $s = A,B,C,D$ to the hills centered at $\mathbf{r}_1,\mathbf{r}_2,\mathbf{r}_3,\mathbf{r}_4$, respectively. We label a trajectory by the symbol sequence according to the sequence of bounces off the corresponding potential hills. This gives a symbolic description in four symbol values with the grammatical restriction that each symbol value is different from its neighbors. Thereby a symbolic dynamics with a branching factor 3 is realized.

To obtain the symbol sequence for a numerical trajectory we place imaginary spheres with radius $d = 1.4$ around the corners of the tetrahedron, i.e., spheres centered at $\mathbf{r_j}$, and monitor in which order the trajectory enters the various spheres. Note that the potential hills do not have a sharp cutoff. Therefore there are very small deflections also for arbitrarily large values of the corresponding impact parameter. Such small deflections are, however, irrelevant for all of our future arguments. Therefore we do not have to care about them, and effectively we can neglect deflections coming from encounters which do not enter the spheres of radius $d = 1.4$ around the corners of the tetrahedron.

III. THE SCATTERING FUNCTION AND ITS FRACTAL STRUCTURE

Next we imagine the following scattering situation. We send in a beam with the incoming momentum prepared in a positive z direction and corresponding to kinetic energy $T = 0.05 < V_0$, and with a constant particle density on the impact parameter plane, which here coincides with the x-y plane. Almost all trajectories leave the potential region after a finite time, and only a subset with measure zero starts exactly on a stable manifold of a localized unstable trajectory and stays in the potential region forever. To each initial condition on this impact parameter plane we assign a symbol sequence according to the corresponding trajectory and in which order it visits the various spheres defined above. If the trajectory does not enter any of these spheres, the symbol sequence is of length zero, i.e., it is empty. We say that such trajectories are of hierarchical level zero.

In the plot of the impact parameter plane in Fig. 1(a) we mark such points of hierarchical level zero as white. In addition there are four disjoint regions R_A,R_B,R_C,R_D of approximately circular shape containing initial conditions which lead to trajectories entering at least one sphere. On hierarchical level 1 we label these four regions by the symbol value of the first sphere entered by the trajectory.

On the next level of the hierarchy there are three subregions inside each region of level 1 where the trajectory enters a second sphere at least. We label such subregions by symbol blocks of length 2 [shown also in Fig. 1(a)] where the second symbol value indicates the second sphere entered. We proceed similarly for higher levels of the hierarchy. For any finite symbol block S of length m we call R_S the subregion of the impact parameter plane consisting of initial conditions belonging to symbol sequences whose first m symbols coincide with S. For each finite allowed symbol block there is exactly one corresponding connected region in the impact parameter plane, and we observe the 1:1 correspondence between S and R_S.

Note that scaling factors can be read off immediately by observing length scales or area scales when going from one level to the next. Because of the grammatical restriction we have always three disjoint subregions of level $i+1$ within each region of level i. In the limit of the level number tending to infinity we obtain in the impact parameter plane a ternary powder fractal F of measure zero. By construction, this fractal represents in the x-y plane the stable manifolds of the unstable trajectories localized forever in the potential region and thus composing the chaotic invariant set (a chaotic saddle [12]), governing the chaotic properties of the scattering. The fractal set F is characterized by a topological entropy ln(3) and a fractal dimension D_F. Assuming that a sufficiently high level i of the set F is covered by a triangle and level $i+1$ can be covered by three similar triangles of factors λ_j, $j = 1,2,3$ smaller in their linear size, the application of the usual similarity argument (see, e.g., Ref. [13]) leads to an implicit equation for the fractal dimension D_F as

$$\lambda_1^{D_F} + \lambda_2^{D_F} + \lambda_3^{D_F} = 1. \tag{4}$$

Comparing levels $i = 3$ and 4 of the hierarchy inside the region R_{AB} [which is shown in Fig. 1(b)], we find only an approximate similarity among the covering triangles, but typical scaling factors can be reasonably well extracted. They are found to be $\lambda_1 = 0.053$, $\lambda_2 = 0.047$, and $\lambda_3 = 0.027$. Substituting these into (4), the estimate $D_F = 0.34 < 1$ is obtained. As a consequence the set F is not intersected by a one-dimensional line of initial conditions in a general position as has been pointed out correctly in Ref. [3].

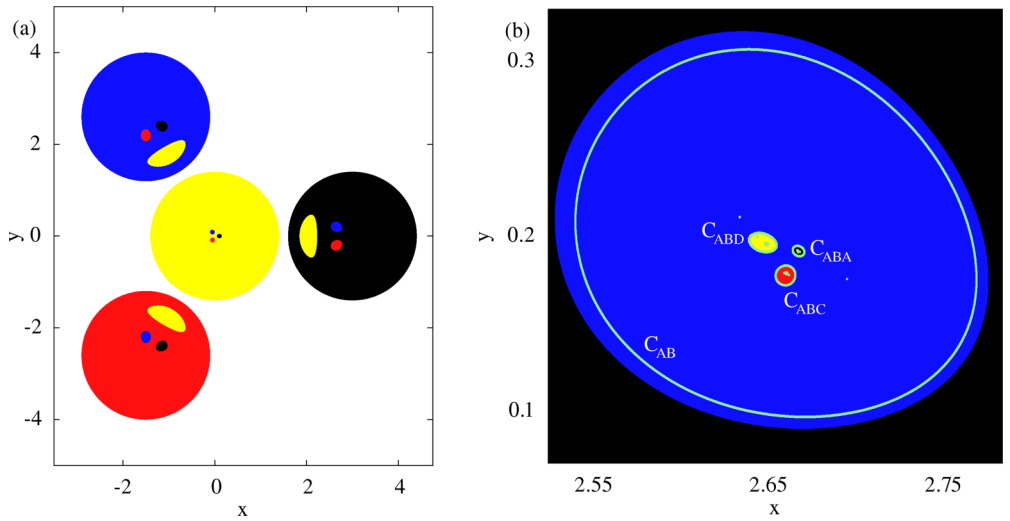

FIG. 1. (Color online) Symbolic partition of the x-y impact parameter plane up to (a) level 2 and (b) level 3 of the hierarchy. The color (gray level in print) indicates the last symbol value of the symbol sequence. Black, blue (dark gray in print), red (light gray in print), and yellow (very light gray in print) stand for the symbol values A, B, C, and D, respectively. (a) The four large regions are the regions of level 1, and the three smaller regions inside of each region of level 1 are the regions of level 2. The color (gray level in print) of the regions of level 2 gives the second symbol value, while the first symbol value is naturally given by the embedding color (gray level in print). (b) Magnification of a part of panel (a) with a further level of the hierarchy included in the coloring (gray level in print). Here the $det = 0$ lines are also plotted. Among these, the line C_{AB} is clearly visible, and C_{ABA}, C_{ABC}, and C_{ABD} can also be distinguished around the boundaries of the regions of level 3.

The whole scattering process maps incoming asymptotes into outgoing asymptotes (with the exception of the subset of measure zero starting on the stable manifold of the chaotic saddle) characterized by the outgoing direction on a sphere. We use on the sphere the usual angular coordinates θ and ϕ for the polar and the azimuthal angle, respectively. In this sense the scattering of the incoming beam defines a map M from the two-dimensional impact parameter plane $\mathbb{R}^2$ with coordinates x and y onto the sphere $\mathbb{S}^2$ of outgoing directions with coordinates θ and ϕ. The set F is the set of singularities of the function M, and it is also the set of intersections of the impact parameter plane with the stable manifold of the chaotic saddle. Thereby it is also the set of initial conditions leading to infinities in the time delay.

For later purposes we need the lines in the impact parameter plane where the determinant of the Jacobian of M is zero (which we call in the following, for short, $det = 0$ lines). In Fig. 1(b) we have included these lines. Note that starting from hierarchical level 2 there is exactly one $det = 0$ line in each region R_S that encircles all the small regions of higher levels lying inside R_S, and the contribution of any other tiny $det = 0$ rings is of negligible length. Then we can also label the $det = 0$ line corresponding to R_S by the same symbol block S. Consequently, we have exactly one line for each allowed symbol block S of length 2 or higher. The $det = 0$ line belonging to the symbol block S will be called C_S in the following. In Fig. 1(b) we show a magnification of a part of Fig. 1(a), with the inclusion of a further level of the hierarchy, to give a pictorial impression of this hierarchical construction. In Fig. 1(b) the curves C_S are included as green lines. C_{AB} is clearly visible, and C_{ABA}, C_{ABC}, and C_{ABD} can also be distinguished at the resolution of the plot. For all other levels the corresponding curves C_S are located similarly near to the boundary of the region R_S.

As can be seen from Fig. 1(b) the various curves C_S of any given finite level of the hierarchy are always separated by gaps. Therefore, the accumulation set of the whole collection of lines C_S for all allowed blocks S consists of the fractal F only. The dimension D_F of F is found to be smaller than one, and the dimension of any curve C_S alone is one. Therefore, we claim, without going to details, the dimension of the collection of all curves C_S is also one.

IV. THE DOUBLY DIFFERENTIAL CROSS SECTION

With the help of the quantities introduced in the last section, the doubly differential cross section, denoted by

$$\frac{d^2\sigma}{d\Omega}(\theta,\phi) = \frac{d^2\sigma}{d\theta\,\sin(\theta)d\phi}(\theta,\phi), \tag{5}$$

can be defined like this. Take an incoming beam with a fixed value of the incoming momentum and a constant particle density on the impact parameter plane. In any classical differential cross section there is a singularity in the forward direction coming from initial conditions with large impact parameters and therefore resulting in little deflection of the corresponding trajectories. It is thus more realistic to use an incoming beam of finite diameter, and then this forward singularity is avoided. By the map M the constant density is mapped on the outgoing sphere $\mathbb{S}^2$. Now divide this density on the outgoing sphere by the total incoming flux. The result is the doubly differential cross section. We can also imagine the graph of the function M in the four-dimensional product space of the domain $\mathbb{R}^2$ and the range $\mathbb{S}^2$ (i.e., the θ-ϕ sphere). This graph carries the incoming constant density. Now let us project the graph with its density on the range. When the incoming density is well normalized then this projected density is again the cross

section. (Note that the range of the map M, i.e., the sphere $\mathbb{S}^2$, is the domain of the doubly differential cross section.)

The map M is not one-to-one, but is locally *smooth* with the exception of a set of points of measure zero, where the set F of scattering singularities sits. For any point (x,y) in the complement of F there belongs one outgoing direction (θ,ϕ), but the inverse is not true. Certain directions are reached from much more impact parameter points than the others. The projection idea makes it clear immediately that the projected density has singularities on projection *caustics* of the graph. They are the rainbow singularities of the cross section. For more information on rainbows see Sec. 5.4 of Refs. [14] and [15]. The rainbows are curves on $\mathbb{S}^2$ where the rank of M drops by one at least and possibly including some points where the rank drops by two. If we cross a smooth line of a rainbow transversely, then the cross section has along this line a one-over-square-root singularity. Note that the integral over such singularities is finite. Therefore such infinities of the cross section do not imply any violation of flux conservation. If we divide the outgoing sphere into a finite number of pixels, like an experimental detector might do, then each pixel receives a finite signal. Of course, pixels containing rainbows or being appropriately close to rainbows exhibit much stronger signals than many neighboring pixels.

Any trajectory making many bounces in the target is not permitted to leave the potential region in an arbitrary direction. We find that there are 12 shadow regions being approximately the projections of the four potential hills cast from the centers of the other potential hills. Then it is natural to label these 12 shadow regions by symbol sequences of length two where a label s_1s_2 belongs to the shadow cast by hill s_2 when illuminated from the center of hill s_1. The shadow of hill s_2 is cast from hill s_1 basically along the (unstable) period-2 orbit bouncing forever between these hills. The symbolic code of this orbit is $s_1s_2s_1s_2\ldots$ or $s_2s_1s_2s_1\ldots$, and there are six such orbit pairs. This observations explains the number of shadow regions and their symbolic codes. The labeled shadows are schematically indicated by black disks in Fig. 2(a).

When we cut these 12 shadows from the sphere then the remainder is multiply connected, and we can characterize closed curves on the sphere by their homotopy class with respect to these 12 holes (the orientations of the curves are irrelevant for our arguments). In the following we will deal with curves which encircle just one of the holes. We naturally label any such curve by the symbol sequence of length two of the encircled hole.

Now we will relate the positions of the rainbows to the shadows. The preimages of the rainbows are exactly the $det = 0$ lines of M shown in the previous section. Therefore we obtain the position of the rainbows simply by mapping these curves C_S. The numerical results are shown in Fig. 2(a). In addition to what is clearly seen in this figure, we have numerically made the following important observation: starting from level 2 of the hierarchy, the images of these lines encircle the shadows

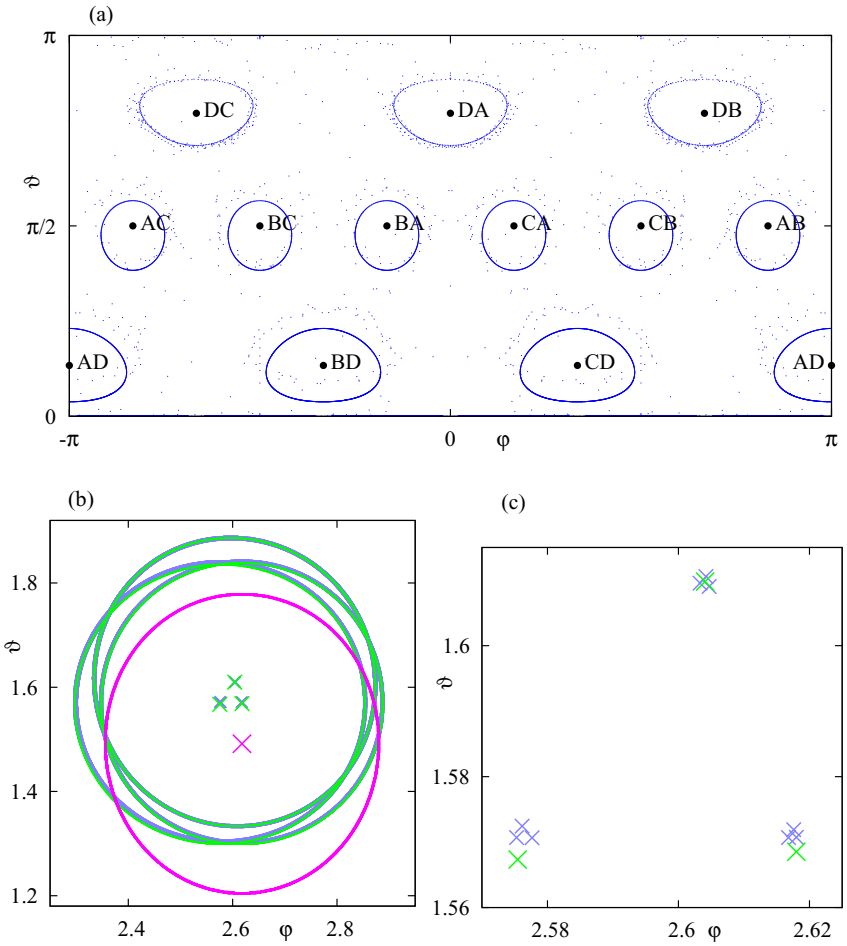

FIG. 2. (Color online) Hierarchical organization of the cross section. (a) Shadow regions shown schematically as black disks along with their symbolic codes, and the images of all the $det = 0$ lines [blue dots (dark gray dots in print)] on the sphere $\mathbb{S}^2$ of outgoing directions. The curves of level 2 can clearly be identified. Higher level contributions appear on this resolution only as scattered points around the shadows. (b) Magnified neighborhood of the shadow AB. The magenta curve (darker gray in print) is the same as the continuous curve around shadow AB in panel (a), i.e., the image of the $det = 0$ line C_{AB}; see Fig. 1(b). The green curves (very light gray in print) are obtained by preparing the $det = 0$ lines C_{BAB}, C_{CAB}, and C_{DAB} with improved resolution and obtaining their image under the map M. The nine curves corresponding to level 4 of the hierarchy with the same last two symbols are marked by light blue (light gray in print). The plot thus explains that the scattered dots seen around shadow AB in panel (a) are signs of the green and the light blue curves but appear as isolated dots due to the lower resolution used there. The centers of mass Z_S of the curves D_S (the images of the curves C_S) are marked by x marks colored correspondingly. Part (c) gives a further magnification where the centers of mass Z_S of level 4 become visible and reflect a ternary organization.

mentioned above. And, more interesting, the symbol block of the shadow encircled coincides with the last two symbols in the symbol block labeling the curve C_S. These observations provide again a hint on the role of the bouncing orbits between the hills and can fully be explained via the arguments used in Ref. [15]. Together with the observations from the last section we have the following result: There is exactly one rainbow curve for each allowed symbol block S of length two or higher. The rainbow curve on $\mathbb{S}^2$ belonging to the symbol block S will be called D_S in the following. The last two symbols of the symbol block S uniquely identify the shadow in $\mathbb{S}^2$ that is encircled by D_S. This observation provides the central idea how the asymptotic observer sees the symbolic description of the dynamics.

Let us reconstruct a smooth image of the fractal F on the domain $\mathbb{S}^2$ of the cross section as follows. We construct the centers of mass Z_S of the curves D_S and plot them on the sphere. Figure 2(b) shows, as an example, the curves D_S with symbol blocks S up to length four that end with AB and the corresponding centers Z_S which lie inside of the shadow AB. The curves D_S and the centers Z_S of levels 2, 3, and 4 are the magenta ($S = AB$), green ($S = BAB, CAB, DAB$) and light blue curves and the similarly colored x marks, respectively. Note that in the resolution of Fig. 2(b) some of the different light blue contributions are not separated from each other. Therefore we show in Fig. 2(c) a magnification of the central part with the centers Z_S. Here we see the initial levels of the hierarchy of the creation of a ternary powder, which is expected to be a smooth image of the ternary powder F in the impact parameter plane. Given that the map M is smooth outside the singularities (where all the $det = 0$ lines lie), the fractal dimension of the set of all Z_S obtained as the limit of an ever increasing length of S (not illustrated here) should be the same D_F as that of the set F in the impact parameter plane. To summarize, the image of the set F seems to be obtained as the collection of the centers of the rainbows in $\mathbb{S}^2$. Thereby, we have found a transfer of the properties of the chaotic saddle's stable manifold to the cross section.

The next important ingredient for the argument on the practical observability of this transfer is the following: Imagine an incoming beam of finite size which illuminates just the region R_S where S is an allowed symbol block, e.g., of length m. Choose the beam such that the neighborhood of the curve C_S is illuminated, but such that no neighborhood of any other curve of equal or lower level of the hierarchy is illuminated. Then the major part of the outgoing signal will be located in the neighborhood of the rainbow curve D_S. The relative weight of higher level regions inside of R_S is small. So in a plot of the corresponding cross section the main contribution appears in the neighborhood of the curve D_S, and therefore we clearly see the last two symbol values of the block S.

Now the idea should be clear how to obtain from asymptotic observations of cross sections the symbol block S of some group of singularities of M. Use a sequence of beams illuminating the regions belonging to the initial subblocks of the block S level by level. In more detail: Let S be the sequence $s_1 s_2 \dots s_{m-1} s_m$. First, illuminate the neighborhood and the interior of curve $C_{s_1 s_2}$ in the impact parameter plane. The corresponding strong signal on the outgoing sphere lies around the rainbow curve $D_{s_1 s_2}$, and the observer can read off the symbol values s_1 and s_2 as the symbol values of the shadow $s_1 s_2$, encircled by $D_{s_1 s_2}$. Next prepare an incoming beam illuminating the neighborhood and the interior of curve $C_{s_1 s_2 s_3}$. The corresponding strong signal on the outgoing sphere lies around the shadow $s_2 s_3$, and its observation allows the asymptotic observer to recover the symbol values s_2 and s_3. Continue along this scheme. Observe on each level the homotopy class of the corresponding main signal in the cross section. This provides a sequence of symbol pairs which reproduces exactly the symbol block S of the chosen group of singularities of M. It is like moving a window of width 2 along the symbol sequence S.

Figure 3 shows a sequence of cross section plots belonging to a sequence of incoming beams, zooming in on a particular group of singularities. First, Fig. 3(a) presents the cross section for a very wide beam which illuminates the whole target. There is a strong signal in the forward direction and some signal on rings around the shadows; compare with Fig. 2(a). The further panels of Fig. 3 give a numerical example for the above procedure, always using rectangular incoming beams.

In Fig. 3(b) we show the cross section belonging to an incoming beam illuminating the neighborhood of R_{AB} [this beam is the rectangle covered by Fig. 1(b)]. Accordingly the signal is strong in the neighborhood of the curve D_{AB}, which encircles the shadow AB. Next, in Fig. 3(c) we use a beam illuminating the neighborhood of R_{ABD} [yellow region in Fig. 1(b)]. Therefore the cross section is large around D_{ABD} encircling the shadow BD. For Fig. 3(d) we illuminate R_{ABDA} giving a strong signal of the cross section near D_{ABDA} encircling the shadow DA. Along this scheme we can zoom in on any grain of the limiting powder fractal and obtain its symbolic description.

In addition we can observe the ratio of the strengths of the signals on consecutive levels of the hierarchy. Thereby we could also obtain the scaling factors λ_1, λ_2, and λ_3 of the hierarchical construction. The branching tree and the scaling factors together are sufficient information to calculate all the measures of chaos of the system. For the thermodynamical formalism for doing this see Ref. [16].

One may notice in Figs. 3(b)–3(d) that the curve carrying the second highest contrast in the cross section (after the most prominent D_S curve) is the image of the boundary of the incoming rectangular beam. According to the continuity of the map M with the exception of singular points, we claim that any curve encircling a group of singularities labeled by a symbol block S has an image in the cross section belonging to the same homotopy class as the corresponding rainbow curve D_S. In other words, one can take an arbitrary curve that just encircles a particular singularity group, labeled by S, in the impact parameter plane and study its image in the cross section in order to obtain the last two symbols in the symbol block S. There exist only two types of curves in the impact parameter plane that both fulfill this condition and have high contrast in the cross section: one "type," represented by only one instance, is the respective C_S curve, and the other type is the boundary of an appropriately prepared incoming beam. When preparing a beam to be appropriate in the latter sense, the following considerations have to be taken into account. First, one should not put the boundary of the beam into the vicinity of a $det = 0$ line other than the respective C_S. This would result

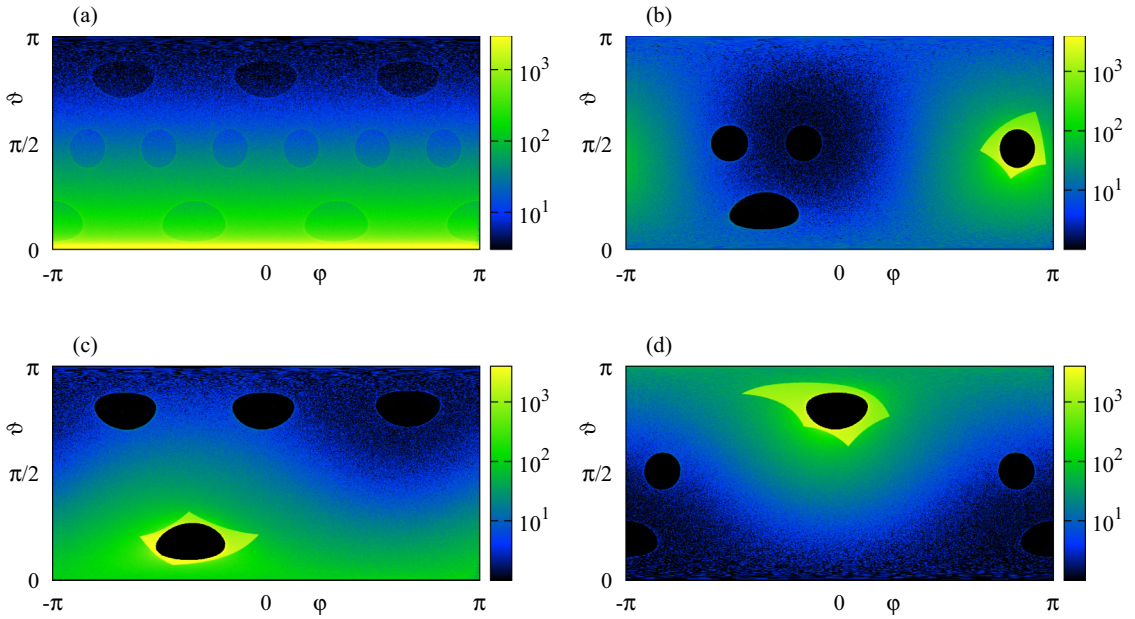

FIG. 3. (Color online) Doubly differential cross section (intensity) for an incoming beam illuminating the whole target in panel (a), whereas in panels (b), (c), and (d) the illuminated regions are rectangles covering R_{AB}, R_{ABD}, and R_{ABDA}, respectively. The color bar (gray scale in print) indicates the intensity on a logarithmic scale. The rainbow caustics visible outside the image of the edge of the incoming rectangular beam always correspond to the $det = 0$ lines (not shown in this figure) of the next level of the hierarchy.

in a serious distortion of the image of the boundary and in high intensities near the rainbow corresponding to the other $det = 0$ line. Second, one should avoid preparing beams that are much smaller than the respective C_S. In such cases, the image of the beam boundary would be even more distorted, and the highest intensities would concentrate near the rainbows corresponding to the next level of the hierarchy. These considerations indicate that the $det = 0$ lines are not essential for the investigation of the homotopy classes, but are essential for providing the relevant geometry and intensities.

It is worth mentioning that the hierarchical organization of the cross section can be unfolded only if the incoming beams are properly chosen. In the case of an *ad hoc* illumination, the different levels become mixed up and the unfolding of the structure might appear to be impossible. It is thus advisable to be acquainted with the organization of the set of singularities in the impact parameter plane before turning to the study of the cross section in numerical studies.

V. DIMENSIONS OF THE FRACTAL OBJECTS IN A GENERAL FORM

Let us consider an autonomous Hamiltonian system with n degrees of freedom where the Poincaré map acts on a

$$N = 2n - 2 \tag{6}$$

-dimensional domain. Let there be a D-dimensional chaotic invariant set in the domain of the map which is a chaotic saddle [12]). (In our tetrahedron system $D < 2$.) In what follows, we will additionally consider the following sets and their dimensions. They are the intersections of the stable manifold of the saddle with two other subsets: with the impact parameter "plane" (this intersection has a dimension D_F) and with a one-dimensional curve in a general position (the dimension of this intersection is denoted by d_F).

Each grain of the chaotic saddle has $N/2$ stable directions and $N/2$ unstable directions. Accordingly, the bundle of stable manifolds of the chaotic saddle has dimension D_s, and the bundle of unstable manifolds of the chaotic saddle has dimension D_u where

$$D_s = D_u = (D + N)/2. \tag{7}$$

The fractal pattern F seen in the $n - 1 = N/2$ dimensional domain of the scattering function is the intersection of this domain with the stable manifold of the chaotic saddle. Using the fact that the codimension of the intersection of two sets is the sum of the components' codimension [17], the dimension of F is

$$D_F = D_s + N/2 - N = D/2. \tag{8}$$

If one would intersect the bundle of stable manifolds with a one-dimensional line, as has been done in Ref. [3], then one would obtain an intersection pattern of dimension

$$d_F = D_s + 1 - N = D/2 + 1 - N/2. \tag{9}$$

We do not obtain intersections for lines in a general position as soon as this number turns out to be negative, i.e., as soon as

$$D < N - 2 = 2n - 4, \tag{10}$$

in agreement with Refs. [3] and [12].

Now let us investigate the dimension of the collection of the $det = 0$ lines. The condition $det = 0$ is a single real condition, therefore it cuts out subsets of codimension 1; i.e., for a scattering function defined on an $n - 1 = N/2$ dimensional domain the individual $det = 0$ subsets are of dimension $n - 2 = N/2 - 1$. We already mentioned for our case of a

powder fractal, but this statement is generally true, that the accumulation set of the whole collection of $det = 0$ subsets coincides with the singularity set, which is of dimension $D_F = D/2$ [see Figs. 1(a) and 1(b)]. When $D_F = D/2 < n-2$, then the dimension of the whole collection of $det = 0$ subsets coincides with the dimension $n-2$ of its individual elements.

Also, the individual rainbows which are the images of individual $det = 0$ subsets are of codimension 1 in the $(n-1)$-dimensional domain of the $(n-1)$-fold differential cross section. The individual rainbows thus have dimension $n-2$. However, in contrast to its preimage, the whole collection of rainbows has a complicated accumulation set, as the various rainbows intersect. Nevertheless, the centers of these individual subsets are organized along a fractal pattern of dimension $D_F = D/2$ [as illustrated by Fig. 2(c)]. Therefore, the collection of all rainbows has at least locally the structure of a Cartesian product of the fractal having dimension $D/2 = D_F$ and of an $(n-2)$-dimensional individual rainbow. Since the dimension of a Cartesian product of two sets is the sum of the dimensions of these sets, the whole collection of rainbows in the scattering cross section has dimension

$$D_\sigma = n - 2 + D/2 = N/2 - 1 + D/2. \qquad (11)$$

Note that this coincides with the result found in Ref. [18] for the case of $n = 2$. In the case $n = 2, N = 2$ we have $D < 2, D_\sigma = D_F < 1$, and, therefore, the rainbows form a fractal pattern on the one-dimensional domain of the cross section too. For $n \geqslant 3, N \geqslant 4$ we have to distinguish the cases $D < 2$ and $D > 2$. In the first case, for $D < 2$ we find $D_\sigma < n-1$; i.e., the dimension of the rainbow set is smaller than the dimension of the domain of the cross section, and we see in the rainbow pattern an image of the fractal structure of the chaotic saddle. For the second case, for $D > 2$, we find $D_\sigma > n-1$, i.e., the dimension of the rainbow set is larger than the dimension of the domain of the cross section, and therefore the rainbow set is space filling in this domain. Then the set of the rainbows does not provide information on the structure of the chaotic saddle. (The inclusion of intensities, which is beyond the scope of the present paper, might provide, however, further signs of fractality, in the sense of multifractal measures [16].)

Now we compare these results with the behavior of the dimension d_F of singularities of the scattering function along a general one-dimensional line. For $n = 2, N = 2$ we always have $d_F = D/2 < 1$, and it provides the information on the chaotic saddle. For $n \geqslant 3, N \geqslant 4$ we have to distinguish the cases $D < N - 2 = 2n - 4$ and $D > N - 2 = 2n - 4$. In the first case $d_F < 0$ and the intersection is empty. In the second case there is an intersection providing information on the chaotic saddle. In the special case $n = 3, N = 4$ we find a complementarity: For $D < 2$ we see the structure of the chaos in the cross section, and for $D > 2$ we see it in the scattering function plotted along a one-dimensional line. Note that the soft potential tetrahedron systems belong to this special case.

VI. CONCLUSIONS

As examples of demonstration we have used an incoming momentum in a positive z direction. For another choice of the incoming momentum the various potential hills might cause shadow effects for the incoming beam, and it does not illuminate some parts of the potential hills which should be illuminated in order to obtain the complete ternary branching tree. Then we can restrict all considerations to some subset of the branching tree and use the self-similarity of fractals to obtain all the information from a subtree.

In the case of a system with three open degrees of freedom the asymptotic observer can reconstruct the symbolic description of the chaotic saddle, a unique sign of chaoticity, from observations of either the scattering function on a two-dimensional domain or of cross sections for appropriate sequences of incoming beams. The symbolic description gives the topology of the chaotic saddle. From the geometry of the fractal set in the scattering function or from the ratio of the signal strength for rainbows of various levels of the hierarchy we obtain the scaling factors. The branching tree and the scaling factors together give the numerical measures of chaos of the system. The asymptotic observer thus obtains the full information on the chaotic saddle by asymptotic observations. In this sense the inverse problem of chaotic scattering is solved for systems with three degrees of freedom, in the present case for an autonomous Hamiltonian system with open degrees of freedom only. This result is a generalization to more degrees of freedom of the result of Ref. [18]. When considering three-degrees-of-freedom systems including one or two closed degrees of freedom, the method described above should work equally well for cases of powder chaos. So far we are not aware of any work on the cross section of such systems. In Refs. [19,20] the rainbow singularities of the cross section have been investigated for systems including closed degrees of freedom where the chaotic set is more complicated and where its stable manifold contains phase space dividing surfaces. In the case of the three-degrees-of-freedom system of Ref. [20] the chaotic set contains a normally hyperbolic invariant set (for these objects see Ref. [21]). Nice examples of rainbows in a system of three open degrees of freedom where the chaotic set is complicated and is not a saddle are presented in Ref. [22].

Similar ideas should work for even higher dimension. For an autonomous Hamiltonian scattering system of n degrees of freedom we have a $2n$-dimensional phase space. The total energy is conserved, and the time of arrival or, equivalently, the position of a particle along the trajectory is irrelevant. Then we naturally arrive at the $N = 2n - 2$ dimensional domain of the relevant Poincaré map. In usual scattering experiments we prepare a set V_1 of $n-1$ of the remaining phase space variables and have a smooth distribution of the $n-1$ ones of the complementary set V_2. Thereby the relevant scattering function lives on a $(n-1)$-dimensional domain of the incoming variables from V_2. We measure the values of the variables from the set V_1 for the outgoing asymptotes. The cross section is the normalized distribution of outgoing trajectories on the space of the variables from V_1. The corresponding scattering function M is again the map from the incoming V_2 space to the outgoing V_1 space. The condition $det = 0$ cuts out $(n-2)$-dimensional surfaces from the V_2 space. Such surfaces are organized according to the intersection pattern of the incoming V_2 space with the stable manifold of the chaotic invariant set. Their images in the outgoing V_1 space are the rainbow singularities of the cross section. They are $(n-2)$-dimensional surfaces. They transport

the organization pattern of the chaotic set into the domain of the $(n-1)$-fold differential cross section where the asymptotic observer can measure it.

Cross sections have the same definition and the same meaning in classical and in quantum dynamics. Therefore we can expect along semiclassical arguments that in quantum systems we can see similar effects as in classical systems up to some limit of resolution given by the quantum uncertainty; i.e., we might see in the quantum counterparts of classically chaotic systems indications of the fractal structures up to some finite level of hierarchy, which, in our case, means a finite hierarchical level of rainbows. Semiclassically the classical one-over-square-root singularity is replaced by the square of an Airy function. The main peak of each Airy contribution has a certain width, and we can only resolve and distinguish the various contributions if their distance is greater than their width. Otherwise, we obtain extremely complicated interference patterns between the various contributions. The corresponding literature [15,18,23–26] treats two degrees of freedom systems where the cross section has a one dimensional domain. For systems with more degrees of freedom we expect analogous behavior perpendicular to the rainbow curves (when there are three degrees of freedom) or surfaces (when there are more of them).

ACKNOWLEDGMENTS

This work has been supported by CONACyT under Grant No. 79988, by DGAPA under Grant No. IG-101113, and by OTKA under Grant No. NK100296. T.T. acknowledges the support of the Alexander von Humboldt Foundation.

[1] J. M. Seoane and M. A. F. Sanjuan, Rep. Prog. Phys. **76**, 016001 (2013).
[2] C. Jung, C. Lipp, and T. H. Seligman, Ann. Phys. **275**, 151 (1999).
[3] Q. Chen, M. Ding, and E. Ott, Phys. Lett. A **145**, 93 (1990).
[4] Y.-C. Lai, A. P. S. de Moura, and C. Grebogi, Phys. Rev. E **62**, 6421 (2000).
[5] M. V. Berry, Phys. Edu. **7**, 1 (1972).
[6] J. Walker, Sci. Am. **259**, 140 (1988).
[7] H. J. Korsch and A. Wagner, Comp. Phys. **5**, 497 (1991).
[8] D. Sweet, E. Ott, and J. A. Yorke, Nature (London) **399**, 315 (1999).
[9] D. Sweet and E. Ott, Physica D **139**, 1 (2000).
[10] D. Sweet and E. Ott, Phys. Lett. A **266**, 134 (2000).
[11] A. E. Motter and P. S. Letelier, Phys. Lett. A **285**, 127 (2001).
[12] Y.-C. Lai and T. Tél, *Transient Chaos* (Springer, New York, 2011).
[13] T. Tél and M. Gruiz, *Chaotic Dynamics* (Cambridge University Press, Cambridge, 2011).
[14] R. G. Newton, *Scattering Theory of Waves and Particles* (Springer, Berlin, 1982).
[15] S. K. Knudson, J. B. Delos, and B. Bloom, J. Chem. Phys. **83**, 5703 (1985).
[16] C. Beck and F. Schlögl, *Thermodynamics of Chaotic Systems: An Introduction* (Cambridge University Press, Cambridge, 1993).
[17] K. Falconer, *The Geometry of Fractals Sets* (Cambridge University Press, Cambridge, 1985).
[18] C. Jung and T. Tel, J. Phys. A **24**, 2793 (1991).
[19] C. Jung, G. Orellana-Rivadeneyra, and G. A. Luna, J. Phys. A **38**, 567 (2005).
[20] C. Jung, O. Merlo, T. H. Seligman, and W. P. K. Zapfe, New J. Phys. **12**, 103021 (2010).
[21] S. Wiggins, *Normally Hyperbolic Invariant Manifolds in Dynamical Systems* (Springer, Berlin, 1994).
[22] F. Gonzalez and C. Jung, J. Phys. A **45**, 265102 (2012).
[23] C. Jung, J. Phys. A **23**, 1217 (1990).
[24] C. Jung and S. Pott, J. Phys. A **23**, 3729 (1990).
[25] J. H. Jensen, Phys. Rev. Lett. **73**, 244 (1994).
[26] J. H. Jensen, Phys. Rev. E **51**, 1576 (1995).